DESIGN STRATEGY FOR THE ROCKING STABILITY OF HORIZONTALLY RESTRAINED MASONRY WALLS

L. Giresini[1]

[1] University of Pisa
Department of Energy, Systems, Territory and Constructions Engineering, Pisa, Italy
linda.giresini@unipi.it

Keywords: Horizontal restraint, rigid block dynamics, resonance, out-of-plane, masonry walls.

Abstract. *This paper investigates the pure rocking of a rigid block with horizontal restraints. The model simulates the behavior of a masonry wall connected to transverse walls and/or steel tie-rods, very frequently adopted as safety measures against seismic actions. From the system rotational stiffness, found for a Winkler-type model and for a single restraint, the resonance conditions of the horizontally restrained blocks are defined. The role of the horizontal restraint can be unilateral (acting only one direction of rotation) and/or bilateral (restraint with similar stiffness in both directions). Real earthquakes or Ricker's wavelets, representing near-fault ground motions, are assumed as input parameters. It is found that in the bilateral case the response is more predictable, as response spectra are monotonic curves whit a reduction of normalized rotation obtained for higher values of restraint stiffness. Moreover, the effect of horizontal restraints is beneficial for the range of frequency parameters valid for typical masonry walls. These considerations allow to define a design strategy to ensure the rocking stability of restrained masonry walls, through a self-centered rocking behavior.*

1   INTRODUCTION

The out-of-plane assessment of masonry walls is generally faced through kinematic approaches [1], [2] or global models where those modes are suggested by a specific deformation pattern of the structure [3]. Nevertheless, a rocking analysis cannot be neglected when assessing the seismic vulnerability of a masonry wall [4]. Rocking behavior is one of the reasons why many ancient structures survived for centuries in highly seismic areas. It can be indeed used as method for stabilizing rigid objects or free structures, in addition to traditional or innovative techniques of dissipation in masonry buildings [5]. Despite their apparent instability under horizontal ground motions, rocking structures exhibit earthquake resistance [6]. The stability condition of the rocking block can be different depending on its boundary conditions: it can be free-standing [7], vertically restrained [8] or horizontally restrained [9]. Moreover, external actions such as thrust of a roof on masonry panels can play a relevant role in the response [10]. The model of a block with horizontal restraints is based on two types of restraints [9]: (i) single spring at a certain depth of the block and (ii) Winkler-type spring bed. Case (i) is representative of antiseismic devices such as steel tie-rods, very frequently used to impede out-of-plane movements of masonry walls [11], [12] . Case (ii) models the role of transverse walls connected to the rocking wall itself. In this paper, the effect of the horizontal restraints under sine pulse, Ricker wavelets and real seismic records is analyzed and discussed. Indeed, the response of the rocking block is particularly sensitive to the input motion. The period of the excitation significantly affects the response and the possibility of collapse: near-field ground motions, that contain long-period directivity pulses, might bring these structures to collapse [13]. Recently, numerical approaches were proposed to identify ground motions capable to cause 'rocking resonance' [14]–[16].

This paper illustrates the dynamics and the system stiffness of horizontally restrained rocking blocks, defining the resonance condition. The dimensionless variables Π, function of the spring bed and the single restraint stiffness, are also derived. Afterwards, the attention focuses on the analysis on a rocking façade under different typologies of pulses. By analyzing the behavior in unilateral and bilateral conditions and widening the analysis for different walls, a design strategy is conceived to reach a rocking behavior for which the response is more controllable and predictable.

2   DYNAMICS AND STIFFNESS OF THE HORIZONTALLY RESTRAINED ROCKING BLOCK

2.1 Equation of motion

The Housner block can be detained by two typologies of restraints: (i) single spring at a certain depth of the block and (ii) closely spaced independent flexible supports (Figure 1). Case (ii) is a simplification of transverse masonry walls connected to the rocking panel. This assumption is an approximation of the real mechanical behavior of transverse masonry walls: indeed, it ignores frictional and multidimensional elasticity effects. Let us assume that in the clockwise (CW) rotation the steel tie-rod is active, as in Figure 1, due to the tensile force acting on it. When the block rotates counter-clockwise (CCW), the tie-rod becomes inactive due to the buckling phenomenon. For what concerns transverse walls, the stiffness is different in CW and CCW rotations: in particular, in CW rotation it should take into account friction forces for the interlocking between the bricks of the rocking wall and those of the transverse walls. Nevertheless, this contribution is neglected and for CW rotation the transverse walls are assumed to not rotate. By contrast, in CCW these are active and offer a stiffening contribution limiting the rocking motion of the wall.

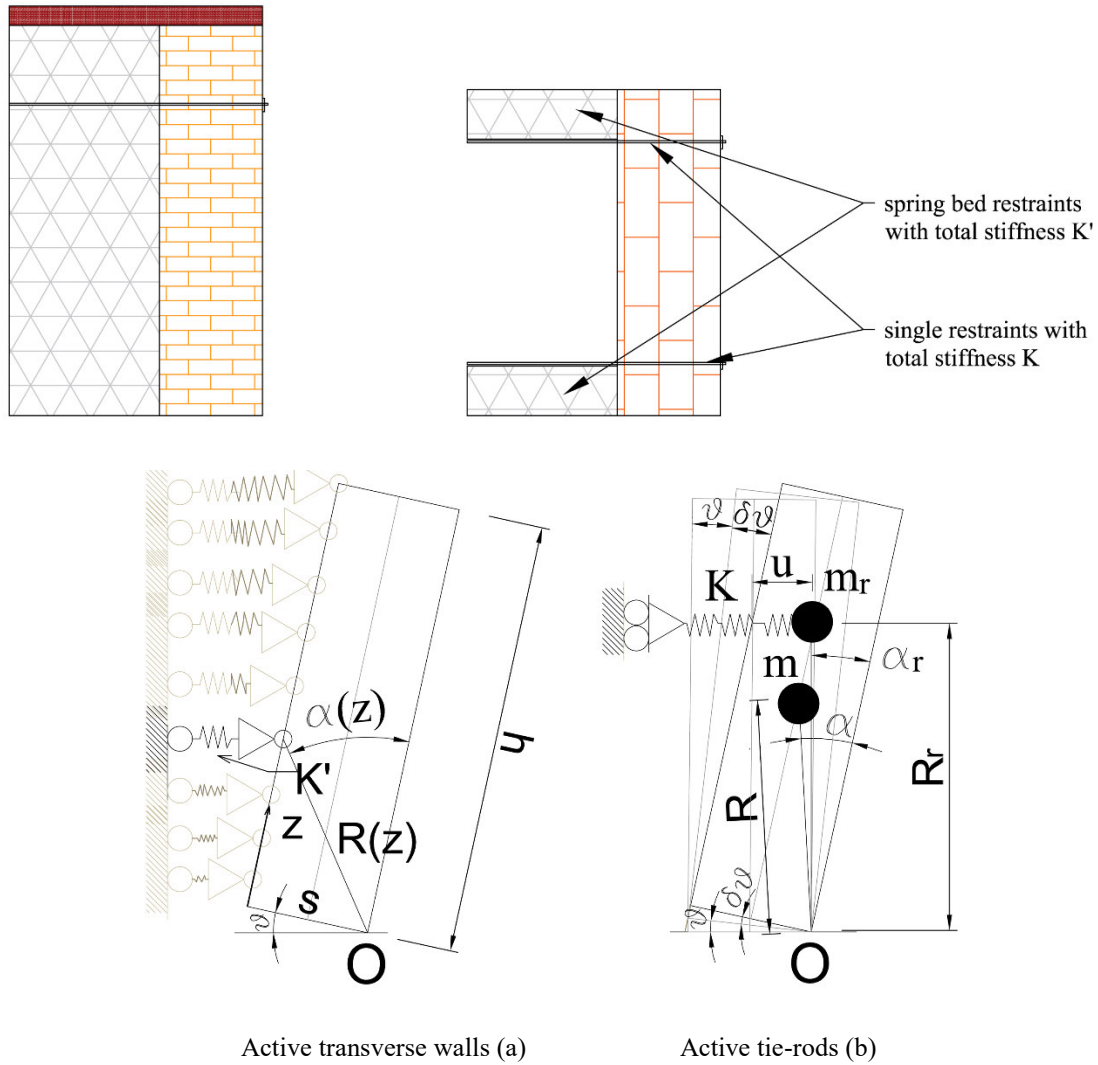Active transverse walls (a)   Active tie-rods (b)

Figure 1: Housner block simulating a masonry wall with transverse walls (a) and steel tie-rods (b). The two structural elements are modeled with closely spaced independent flexible supports smeared out through the depth of the block (a) and single spring with the radius vector βR (b).

The complete equation of motion of the block restrained by a single restraint (of stiffness K) and by a spring bed (of stiffness K') is:

$$I_0\ddot{\vartheta} + sgn(\vartheta)mgR \sin A_\vartheta + \tag{1}$$

$$+sgn(\vartheta)\, K\beta^2 R^2 \cos A_{r,\vartheta}\ [sin\,\alpha_r - \sin A_{r,\vartheta}] + sgn(\vartheta)\, K'\bar{h}\left(A + \frac{B\bar{h}}{2} + \frac{C\bar{h}^2}{3}\right)$$

$$- m\,\ddot{u}_g R \cos A_\vartheta = 0$$

where:

$$A_\vartheta = \alpha - sgn(\vartheta)\vartheta \tag{2}$$
$$A_{r,\vartheta} = \alpha_r - sgn(\vartheta)\vartheta$$

α is the block radius vector, whereas α_r is the single spring radius vector. Moreover, $\bar{h}$ is the height along which the spring bed is effective. This value may obviously be lower than the block height h. $\ddot{u}_g$ is the seismic excitation and β defines the single spring position.

This equation can be also expressed in function of the frequency ratio $p^2 = mgR/I_0$ by dividing it by I_0:

$$
\ddot{\vartheta} = -sgn(\vartheta)\, p^2 \left\{ \sin A_\vartheta + \frac{K\beta^2 R}{mg} \cos A_{r,\vartheta} \left[sin\, \alpha_r - \sin A_{r,\vartheta} \right] \right.
$$
$$
\left. + 2\cos\alpha\, \frac{K'}{mg} \left(A + \frac{B\bar{h}}{2} + \frac{C\bar{h}^2}{3} \right) \right\} + p^2 \frac{\ddot{u}_g}{g} \cos A_\vartheta
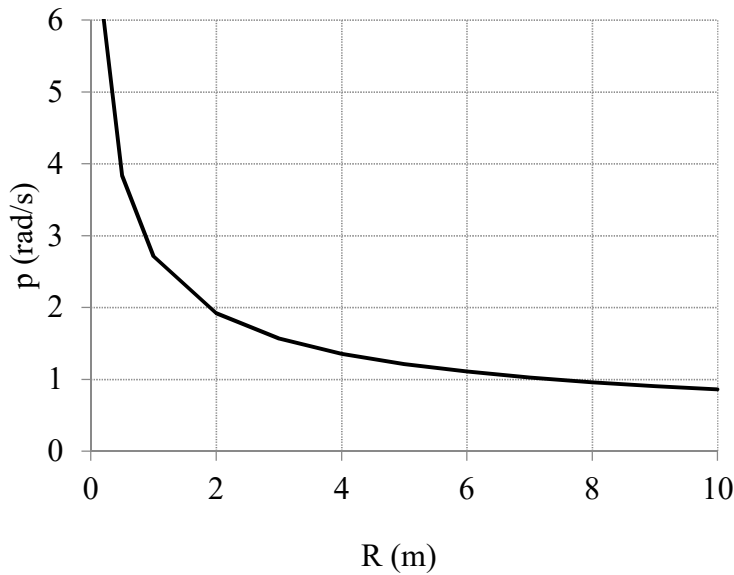$$

(3)

where the terms multiplied by K' are:
$A = sgn(\vartheta)\, s^2 \sin\vartheta\, \cos\vartheta\, (1 - \cos\vartheta)$;
$B = s\, (\sin^2\vartheta\, \cos\vartheta - \cos^3\vartheta + \cos^2\vartheta)$;
$C = sgn(\vartheta) \sin\vartheta\, \cos^2\vartheta$.

For values of radius vectors valid for masonry walls, namely $0 < R < 10$ m, where the larger values are typical of large façades of monumental buildings, the frequency ratio p, assuming rectangular block, varies as displayed in Figure 2.

Frequency ratio p:
$$p = \sqrt{mgR/I_0}$$

For rectangular blocks:
$$p = \sqrt{\frac{mgR}{\frac{4}{3}mR^2}} = \sqrt{\frac{3g}{4R}}$$

Figure 2: Frequency ratio p for rectangular blocks in the range of interest of R values valid for masonry façades.

The integration of Equation (2) expresses the time-history response of the restrained rocking block, which is function of the following parameters:

$$
\vartheta = f\left[p, \alpha, \alpha_r, \frac{K\beta^2 R}{mg}, \frac{K'}{mg} \left(A + \frac{B\bar{h}}{2} + \frac{C\bar{h}^2}{3} \right) \right]
$$

(4)

Those terms depend only on the geometry of the block and on the type of restraints, with the exception of A, B, C (Equation (3)) that need to be further modified as reported in the following paragraph.

2.2 Ricker wavelets and derivation of dimensionless terms for the restrained block

The seismic action, enclosed in the term $\ddot{u}_g$ of Equation (2), generally has different frequency contents and amplitudes. Nevertheless, several authors considered the rocking response to pulses described as simple trigonometric functions and explained why rocking structures are particularly vulnerable to pulse-type earthquakes. In [17], it is observed that small blocks overturn with short period pulses, whereas larger blocks overturn due to the long-duration pulse. The detrimental role of long-period pulses inherent in near-fault ground motions is also observed [18]. The Authors consider that under cycloidal pulses a free-standing block can overturn with two distinct modes: (1) by exhibiting one or more impacts; and (2) without exhibiting any impact. For the second mode, it can be determined a safe region that is located on the acceleration-frequency plane above the minimum overturning acceleration spectrum. The shape of this region depends on the restitution coefficient.

For pulse-type earthquakes, the use of dimensionless variables is very advantageous.

The Ricker wavelet [19] or its time derivative well approximate coherent pulses of several pulse-like ground motions [20]:

$$\psi(t) = a_p \left(1 - \frac{2\pi^2 t^2}{T_p^2}\right) e^{-\frac{1}{2}\left(\frac{2\pi^2 t^2}{T_p^2}\right)} \tag{5}$$

where a_p is the amplitude of the acceleration pulse. The value of $T_p = \frac{2\pi}{\omega_p}$ is the period that maximizes the Fourier spectrum of the wavelet, being ω_p the circular frequency of the acceleration pulse. A relevant value correlated to those parameters is the characteristic length scale of the ground excitation. This parameter, $L_p = a_p T_p^2$, gives a measure of the persistence of the most energetic pulse capable to generate inelastic deformation.

If one considers then pulse-type excitations, the response can be expressed in function of:

$$\vartheta = f\left[p, \alpha, K, K', a_p, \omega_p, g\right] \tag{6}$$

assuming that, for the sake of simplicity, $\alpha = \alpha_r$ (slender blocks). The number of dimensionless products that completely describe the motion, according to the Vashy-Buckingham Π theorem [8], [21], is given by the number of variables (8) minus the number of reference dimensions (2, namely the time and the length). One has then 6 dimensionless products, which are:

$$\Pi_\vartheta = \vartheta; \ \Pi_\omega = \frac{\omega_p}{p}; \ \Pi_\alpha = \tan\alpha; \ \Pi_g = \frac{a_p}{g}; \ \Pi_K = \frac{K\beta^2 R}{mg}; \ \Pi_{K'} = \frac{K'R^2}{mg} \tag{7}$$

The validation of a MATLAB code used herein to generate the rocking curves and spectra solve a 4th-5th order is performed by comparing the results with those obtained by [8]. The integration of Equation (3) is performed with the Runge-Kutta method [22].

By considering the following dimensionless parameters:

$$\Pi_\omega = 1.0; \frac{\Pi_g}{\Pi_\alpha} = 2; \ \Pi_a = 0.176; \ \Pi_\gamma = 0 - 2; \ \Pi_K = \Pi_{K'} = 0, \tag{8}$$

it is possible to obtain rocking spectra. In Equation (8), Π_γ refers to a rocking frame, made by a set of N columns of mass m_c and a cap beam of mass m_b. The frequency ratio of a rocking frame is given by $\hat{p} = p\sqrt{(1+2\gamma)/1+3\gamma}$, where $\gamma = m_b/(Nm_c)$ [23]. The dimensionless parameter Π_γ correspond to the value of γ. The obtained rocking spectra are displayed in Figure 3.
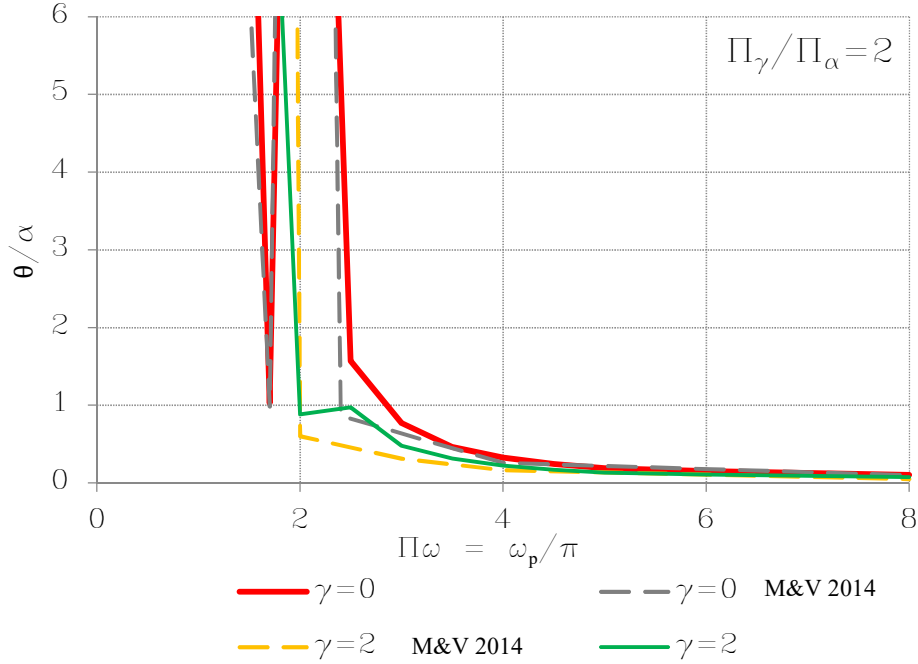

Figure 3: Rocking spectra for $\Pi_\omega = 1.0$; $\frac{\Pi_g}{\Pi_\alpha} = 2$; $\Pi_a = 0.176$; $\Pi_\gamma = 0 - 2$, results compared with Figure 3 of [8].

2.3 System rotational stiffness for smeared and single horizontal restraints

By expressing the work made by the springs in the two models, the resisting moment-rotation relationship is obtained, which is for case (i) [9]:

$$M_r(\vartheta) = mgR \sin(\alpha - \vartheta) + K\beta^2 R^2 \cos(\alpha - \vartheta) \left[\sin\alpha - \sin(\alpha - \vartheta) \right] \qquad (9)$$

By assuming a constant spring stiffness K' smeared out through the whole depth of the block, the dimensionless resisting moment-rotation relationship for the spring bed model is [9]:

$$M_r(\vartheta) = mgR \sin(\alpha - \vartheta) + K'h \left(A + 2BR \cos\alpha + \frac{4CR^2 \cos^2\alpha}{3} \right) \qquad (10)$$

where:

$$
\begin{aligned}
A &= sgn(\vartheta)\, s^2 \sin\vartheta\, \cos\vartheta\, (1 - \cos\vartheta); \\
B &= s\, (\sin^2\vartheta\, \cos\vartheta - \cos^3\vartheta + \cos^2\vartheta); \\
C &= sgn(\vartheta) \sin\vartheta\, \cos^2\vartheta
\end{aligned}
\qquad (11)
$$

The function $sgn(\vartheta)$ expresses the sign $\pm$ depending on the rotation sign, clockwise or counterclockwise. Let us assume here a positive rotation. Equations (9) and (10) are valid for any

rotation, whereas for small rotation, for which $\sin \vartheta \cong \vartheta$, $\cos \vartheta \cong 1$ and second order terms are neglected, the system rotational stiffness reads [9]:

$$K_{sys} = mgR\cos\alpha \left(\frac{K\beta^2 R}{mg}\cos\alpha - 1\right) \tag{12}$$
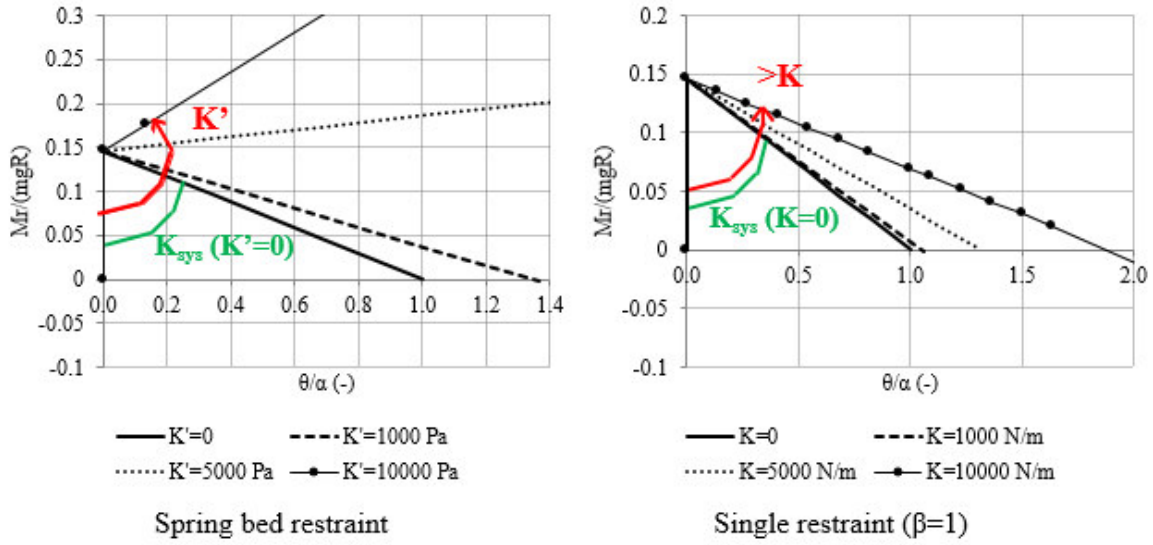
for the single spring model.

Figure 4: System rotational stiffness K_{sys} in the dimensionless resisting moment-rotation relationship and curve variation with increased values of spring bed stiffness K' and single spring stiffness K (masonry wall with $\gamma=18$ kN/m³, $\alpha=0.15$ rad and $R=2.0$ m), Equations (9) and (10).

In case of the spring bed model one has:

$$K'_{sys} = mgR \cos \alpha \left(\frac{8}{3}\frac{K'R^2}{mg}\cos^2 \alpha - 1\right). \tag{13}$$

Both Equations (13) and (14) allow to express the moment-rotation law in a simplified way:

$$M_r(\vartheta) = M_r(0) + K_{sys}\,\vartheta \tag{14}$$

$$M_r(\vartheta) = M_r(0) + K'_{sys}\vartheta$$

where $M_r(0) = mgR \sin\alpha$. The rotational stiffness K_{sys} or K'_{sys} is the slope of the line in Figure 4, increasing for higher values of either K or K'.

In the hypothesis of small rotations, one can easily define the value of the single spring stiffness in order to equate the two system rotational stiffness, by equating Equation (12) to Equation (13):

$$K_{sys} = K'_{sys} \rightarrow K = \frac{8}{3\beta^2}K' \cdot R\cos\alpha \tag{15}$$

Higher the spring bed stiffness, higher the stiffness of the single restraint. The latter is also proportional to the radius vector and to the cosine of the slenderness ratio. For what concerns the single spring position, lower the position (lower β), higher its stiffness value, as expected.

3 RESONANCE CONDITION

The resonance condition is obtained when the rotational frequency of the rocking block equates that of the excitation, namely $\omega_r = \omega_p$. In particular, for the case of spring bed the square of rotational frequency is:

$$\omega_r^2 = \frac{K'_{sys}}{I_0} = \frac{mgR\cos\alpha\left(\frac{8K'R^2}{3\ mg}\cos^2\alpha - 1\right)}{I_0} = p^2\cos\alpha\left(\frac{8}{3}\frac{K'R^2}{mg}\cos^2\alpha - 1\right). \tag{16}$$

Therefore:

$$\omega_r = p\sqrt{\cos\alpha\left(\frac{8}{3}\frac{K'R^2}{mg}\cos^2\alpha - 1\right)}\ \ M_r(\vartheta) = mgR\sin(\alpha\text{-}\vartheta) + \tag{17}$$
$$K\beta^2 R^2\cos(\alpha\text{-}\vartheta)\left[\sin\alpha\text{-}\sin(\alpha\text{-}\vartheta)\right].$$

For the single horizontal restraint one has:

$$\omega_r^2 = \frac{K_{sys}}{I_0} = \frac{mgR\cos\alpha\left(\frac{K\beta^2 R}{mg}\cos\alpha - 1\right)}{I_0} = p^2\cos\alpha\left(\frac{K\beta^2 R}{mg}\cos\alpha - 1\right) \tag{18}$$

and

$$\omega_r = p\sqrt{\cos\alpha\left(\frac{K\beta^2 R}{mg}\cos\alpha - 1\right)}. \tag{19}$$

Both circular frequencies linearly depend on the frequency parameter p. For a slender column, $\cos\alpha \cong 1$ and the circular frequencies at resonance become:

$$\omega_{r,sm} = p\sqrt{\left(\frac{8}{3}\frac{K'R^2}{mg} - 1\right)}\ ; \omega_{r,single} = p\sqrt{\left(\frac{K\beta^2 R}{mg} - 1\right)}\ . \tag{20}$$

That, in dimensionless terms, can be expressed as:

$$\Pi_{\omega,sm} = \sqrt{\frac{8}{3}\Pi_{K'} - 1}\ ; \Pi_{\omega,single} = \sqrt{\Pi_K - 1}, \tag{21}$$

respectively for smeared and single restraints. It is worthy to notice that these dimensionless terms do not depend on the slenderness ratio α.

4 DYNAMIC RESPONSE WITH UNILATERAL OR BILATERAL RESTRAINTS

The dynamic response is strongly different if unilateral (mainly acting in one side of the block) or bilateral restraints (stiffness equal or at least of the same order of magnitude for both directions).
Let us assume a masonry façade connected with transverse walls, with analysis parameters reported in Table 1. The wall is the main façade of the Santa Gemma Church in Goriano Sicoli (L'Aquila), whose damage suggested a rocking motion during the L'Aquila earthquake [9].

To evaluate the influence of the horizontal restraints in the motion, the façade is subjected first to a sin pulse type action and then to a seismic-type excitation. The façade has two configurations: (a) spring bed modeling transverse walls acting only in one direction (non linear, NLin) and (b) spring bed with the same stiffness as that of the transverse walls in the two directions (linear, Lin).

A parametric analysis is performed by assuming a range of spring bed stiffness values K' between 0 and 1E10 N/m^2 and three types of input action: sin pulse, real seismic records, Ricker wavelets. For all the analyses the restitution coefficient adopted is that of Housner, depending only on the slenderness ratio α [7].

Parameter	Value	Definition
R (radius vector)	5.726 m	Geometric survey
α (slenderness ratio)	0.0778 rad	Geometric survey
s (thickness)	0.89 m	Geometric survey
e (restitution coefficient)	0.9909	Derived by $e = 1 - \frac{3}{2}\sin^2\alpha$ [7]
L (depth of the wall)	10.10 m	Geometric survey
γ_{mas} (specific weight)	18 kN/m^3	Literature value (brick masonry, from [2])
E_y (vertical direction)	1700 MPa	Masonry elastic modulus (in-situ flat jack test)
E_x (horizontal direction)	2125 MPa	Derived by E_y/0.8 [24].
K'_{TOT} (transverse stiffness of the spring bed)	5.07E9 N/m^2	Derived as in [9].

Table 1: Geometric and mechanical parameters of the analyzed masonry façade.

4.1 Response to sine pulse-type action

The pulse has an acceleration $a = 2.5 \tan(\alpha)\, g \cdot \sin(\omega t)$ and duration of 1 sec, after which the motion is on free vibration. The response is displayed in Figure 5.

The frequency of the pulse is $\omega = 5.8$ rad/sec. The dynamic response is monitored for 10 seconds.

In the non-linear case (Figure 5a), the motion is oscillatory up to K' values of about 1E6 N/m^2, whereas for higher values the rebound effect is clear. The rotation amplitude slightly decreases when the motion is oscillatory and the frequency increases for higher K' values. This consideration is also valid for the linear case (Figure 5b), where the response is more controllable being symmetric. In this case the reduction of the rotation amplitude and of the vibration period are more evident. For instance, a value of K' value of 1E6 N/m^2 is needed to obtain a reduction by 40% of the initial maximum rotation amplitude for the case without restraints. Correspondingly, a tripled frequency of vibration occurs. The measured value of transverse walls stiffness is about 5.07E9 N/m2 (calculated in elastic range). For this value, if one assumes the linear case, the normalized rotation is close to zero (Figure 5b). By contrast, in case of unilateral restraint, the maximum rotation amplitude is about the same as that without restraints ($\cong 0.7$) and the frequency of vibration is nearly the same ((Figure 5a).
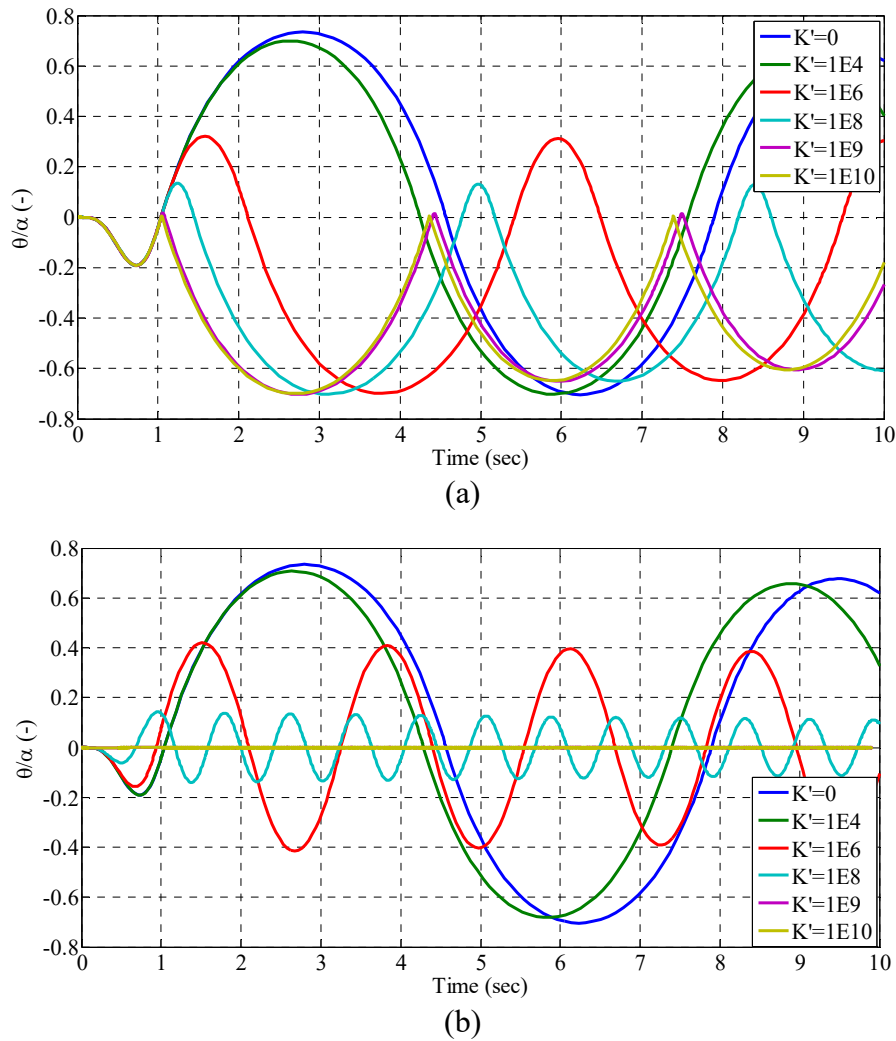
Figure 5: Normalized rotation time-history of the façade under a sin pulse-type action: (a) unilateral spring bed simulating transverse walls; (b) bilateral spring bed. Stiffness values are expressed in N/m².

4.2 Response to real seismic records

In this paragraph the response of the façade subjected to real earthquakes is discussed. The façade undergoes seismic records that it actually experienced during the L'Aquila main shock (Italy, 2009), whose acceleration time-histories are featured in [9]. The response of the façade is similar to that of the sine pulse for both unilateral and bilateral restraints. Indeed, if one considers the real case, that is unilateral restraints (spring bed with $\bar{h} = 4.90 \neq h$), the overturning is not predictable, as for some K' ranges (e.g., $1E6 < K' < 1E7$ N/m², and $K' > 1E11$ N/m² - AQV record, Figure 6a) the façade overturns. The overturning phenomenon is due to a rebound effect due to the sensitive difference between restraints stiffness in the two directions of rotation. By contrast, when bilateral restraints participate to the motion, the behavior is much more predictable: a decreasing maximum amplitude ratio ϑ_{max}/α can be observed for higher stiffness values (Figure 6b). This monotonic behavior suggests a design strategy for anti-seismic devices, based on reaching similar values of stiffness in the two directions of rotation.
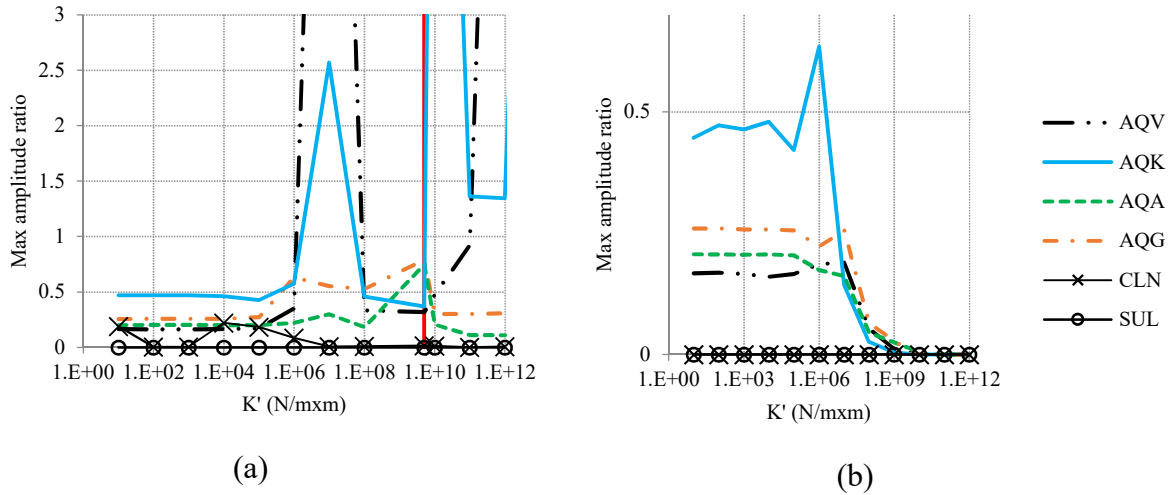
Figure 6: Response of the masonry façade to real seismic records: (a) unilateral spring bed; (b) bilateral spring bed [9].

4.3 Response to Ricker wavelets

The façade frequency parameter p is equal to 1.134 rad/s and $\Pi_a = 0.078$. To widen the results in case of Ricker wavelets, a parametric analysis is performed for the dimensionless parameters $\Pi_\omega = 0.5 - 8$ and $\frac{\Pi_g}{\Pi_a} = 2 - 3$. Only the spring bed restraint is considered, varying the dimensionless $\Pi_{K'}$ values from 0 to 10. An oscillation motion is observed for the free rocking façade ($\Pi_{K'} = 0$) and in case of bilateral restraints, as shown in the response spectra of Figure 7a, the curves are monotonic and the overturning domain reduces for higher $\Pi_{K'}$ values. By contrast, when restraints act unilaterally (in only one direction it is $\Pi_{K'} \neq 0$, in the other one it is zero), the response is not so predictable, as for some values of $\Pi_{K'}$ (e.g. $\Pi_{K'} = +1.0$, Figure 7), there is not a monotonic trend (Figure 7b).
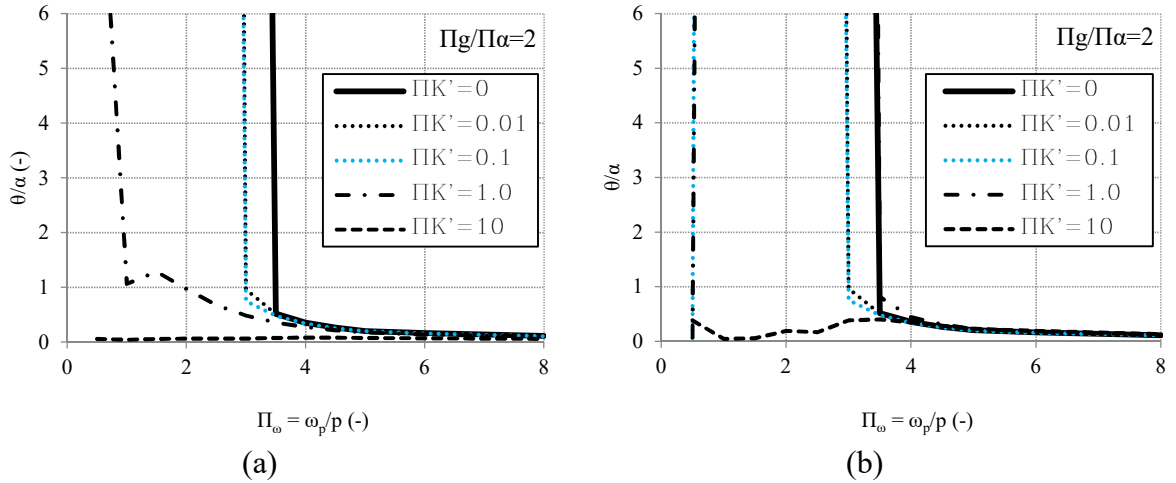

Figure 7: Rocking spectra of the façade under Ricker wavelets with $\frac{\Pi_g}{\Pi_a} = 2$: (a) bilateral case and (b) unilateral case.

Moreover, the beneficial role of horizontal restraints is valid only for a range of Π_ω lower than a limit value, in this case about 3.8 for both cases, inasmuch for higher values the response with and without horizontal restraints tends to be similar. An analogous results was found for the rocking response of panels with vertical restraints [8].
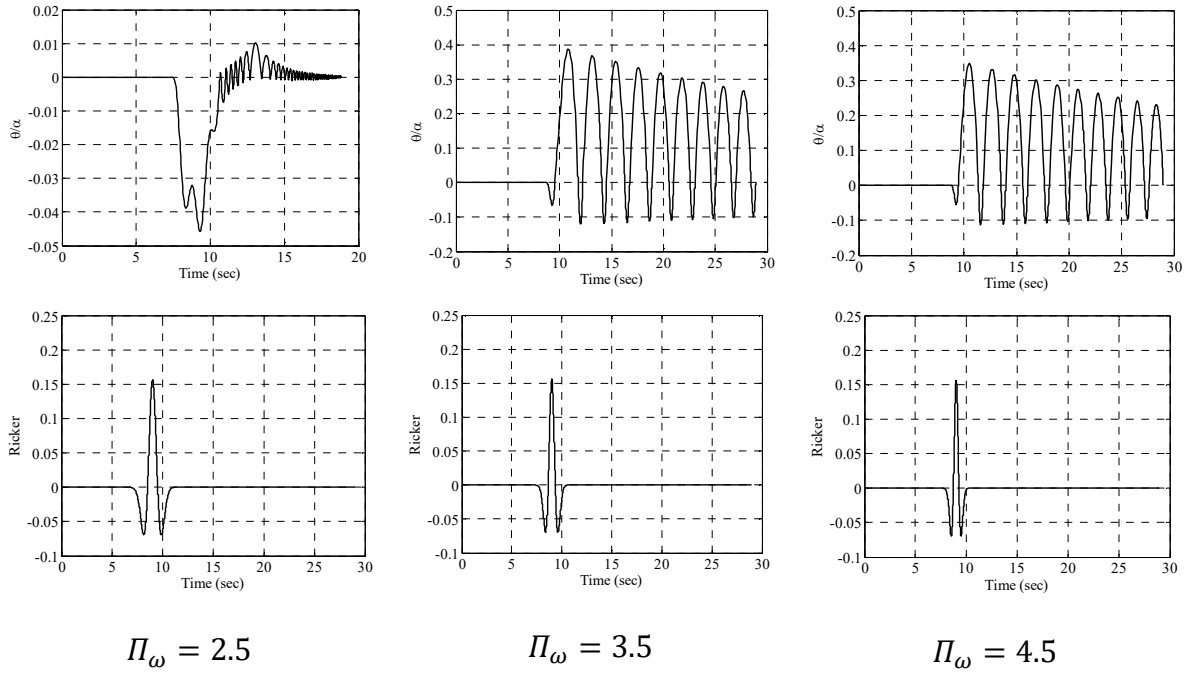
Figure 8: Response in unilateral case of the masonry façade to Ricker wavelets with $\frac{\Pi_g}{\Pi_\alpha} = 2$: $\Pi_{K\prime} = +10.0$.
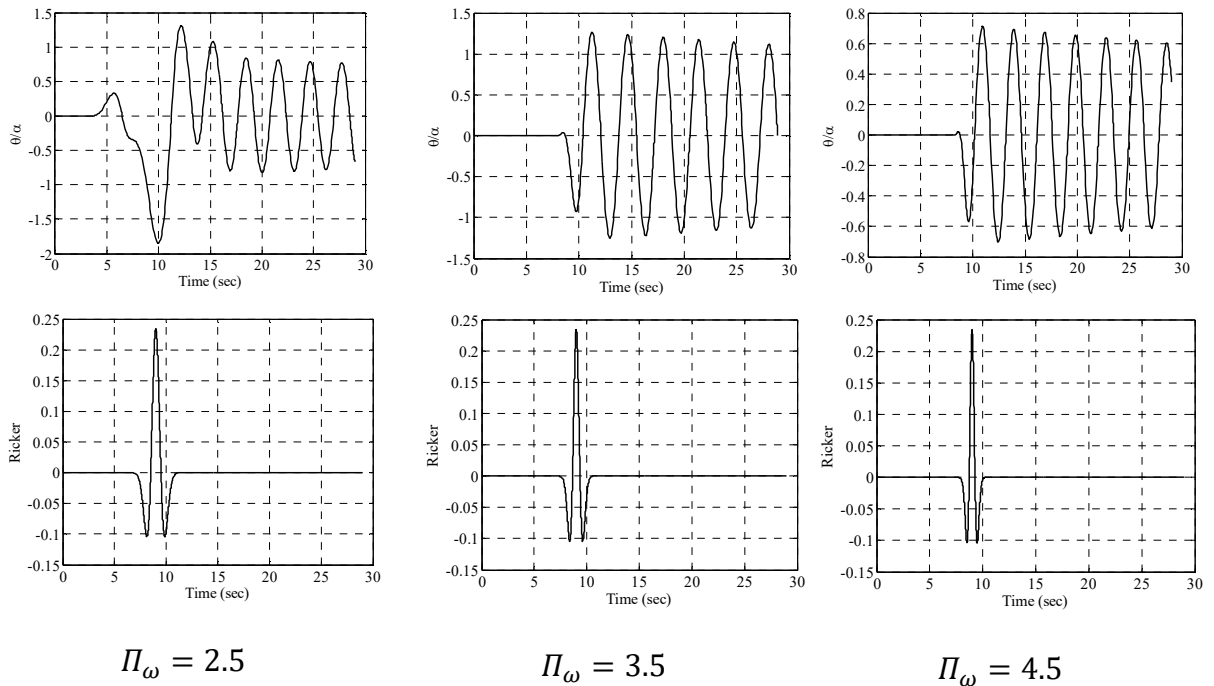

Figure 9: Response in bilateral case of the masonry façade to Ricker wavelets with $\frac{\Pi_g}{\Pi_\alpha} = 3$: $\Pi_{K\prime} = 1$. Resonance condition for $\Pi_\omega = 1.28$.

When a unilateral restraint is assumed, for $\frac{\Pi_g}{\Pi_\alpha} = 2$ the time-history rotation displayed in Figure 8 highlights that the rebound effect is clear but the value of stiffness is not such as to cause overturning.

If the same analysis is carried out by increasing the excitation amplitude to $\frac{\Pi_g}{\Pi_\alpha} = 3$, lower the spring bed stiffness value, higher the amplitude for the same frequency parameter Π_ω (Figure 9 for $\Pi_{K'} = 1$ and Figure 10 for $\Pi_{K'} = 10$) in case of bilateral restraints.

$$\Pi_\omega = 2.5 \qquad \Pi_\omega = 3.5 \qquad \Pi_\omega = 4.5$$
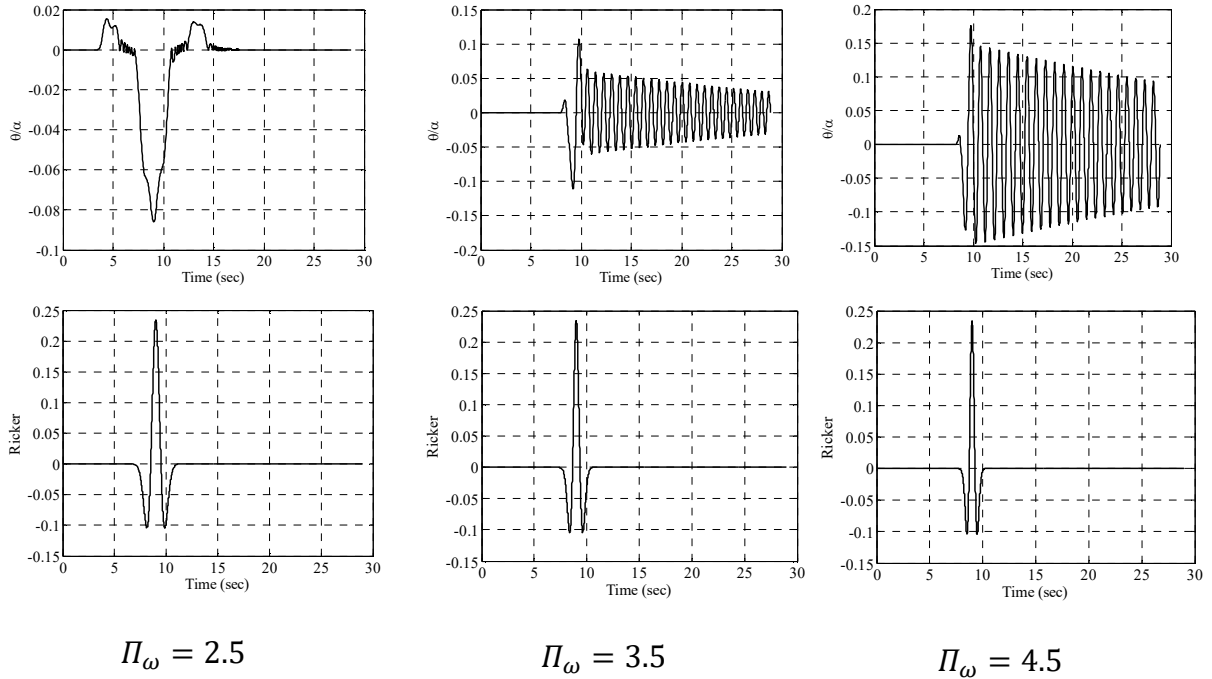
Figure 10: Response in bilateral case of the masonry façade to Ricker wavelets with $\frac{\Pi_g}{\Pi_\alpha} = 3$: $\Pi_{K'} = 10$. Resonance condition for $\Pi_\omega = 5.04$.
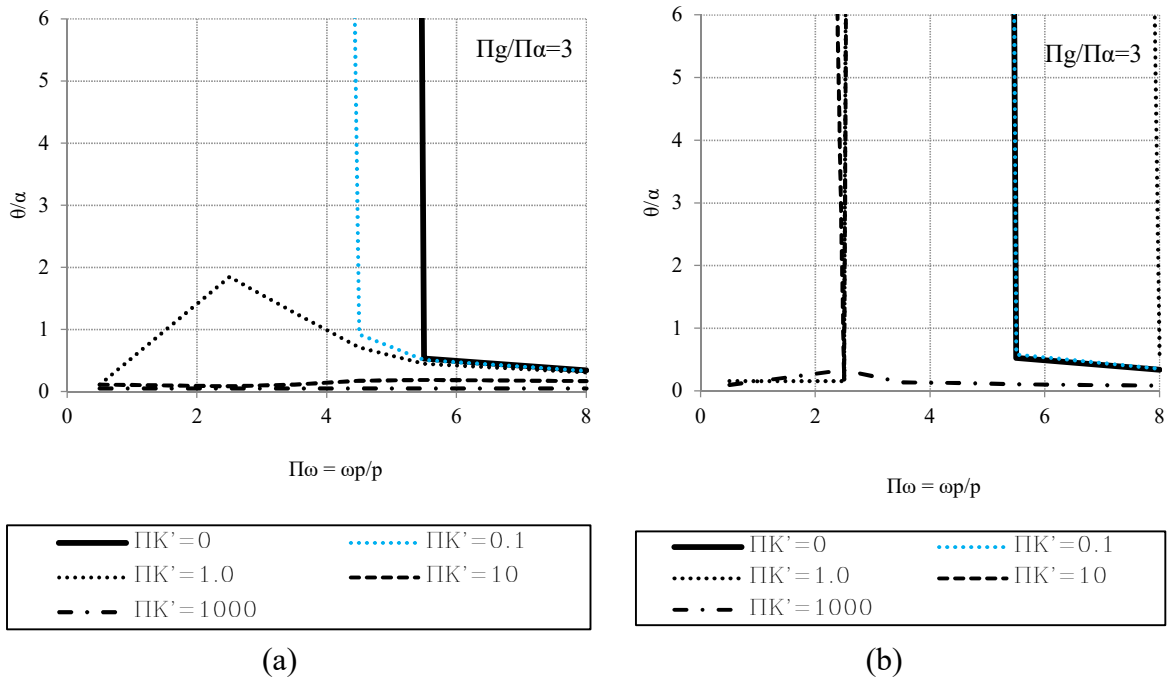

(a)   (b)

Figure 11: Rocking spectra of the façade under Ricker wavelets with $\frac{\Pi_g}{\Pi_\alpha} = 3$: (a) bilateral case and (b) unilateral case.

The value of Π_ω in resonance condition increases when higher stiffness value of $\Pi_{K\prime}$ are assumed. However, an oscillatory motion is always registered for the bilateral restraints, while for unilateral restraints the difference of stiffness depending on the rotation sign causes the block overturning for rebound effect. In Figure 11 the response spectra of the façade under Ricker wavelets with Π_g/Π_α =3 are displayed. As occurred for the lower value of excitation amplitude, the response in the bilateral case is predictable with a monotonic trend, while in the unilateral case for some $\Pi_{K\prime}$ values the façade overturns. In the case of bilateral restraints, the Π_ω value above which the restraints are not effective is about 5.5 (Figure 11a). In the unilateral case, the range of $\Pi_{K\prime}$ included between 2.5 and 5.5 is associated to unstable conditions.

5   DESIGN STRATEGY: TARGET POINTS AND CONFIDENT RANGE

The use of Equation (15) is related to a possible design strategy for anti-seismic devices (such as steel tie-rods), whose stiffness is K. The following procedure can be adopted to define a K value to have the same (or a similar value) system stiffness as that of the spring bed model. Once that the transverse stiffness of the wall is defined, depending on the radius vector and the slenderness ratio of the rocking wall, it is straightforward to determine the system stiffness from Equation (13). In a graph, valid for a specific value of slenderness ratio α, the radius vector R of the block under examination intersects a curve (Equation (12)) describing the dimensionless system stiffness (on the ordinates) in function of R. This curve corresponds to the target value of the single restraint stiffness K (Figure 12). From this value, it is therefore possible to easily calculate the diameter of the steel tie rods [9]. The position of the single restraint, denoted with β, is given by the curve itself (Equation (12)).

For instance, if one has a transverse walls stiffness equal to K'=5E7 N/m^2, R=4 m and α =0.15 rad, to get roughly the same system stiffness, a single restraint stiffness has to be about 1E8 N/m (Figure 13).

From these parametric curves one can obtain range of values of the single restraints stiffness associated to steel tie-rods able to ensure a predictable behavior of the masonry walls, searching for an oscillatory motion.
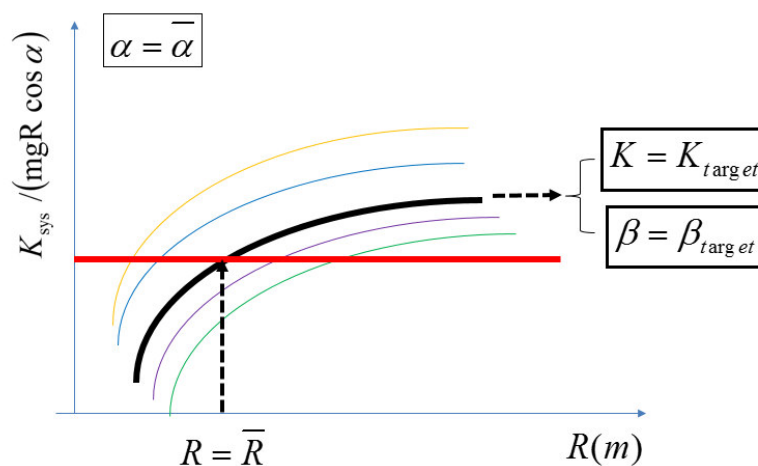

Figure 12 Procedure to define the value of the single restraint stiffness K that equates the system stiffness $Ksys$ depending on an assigned spring bed stiffness K'.
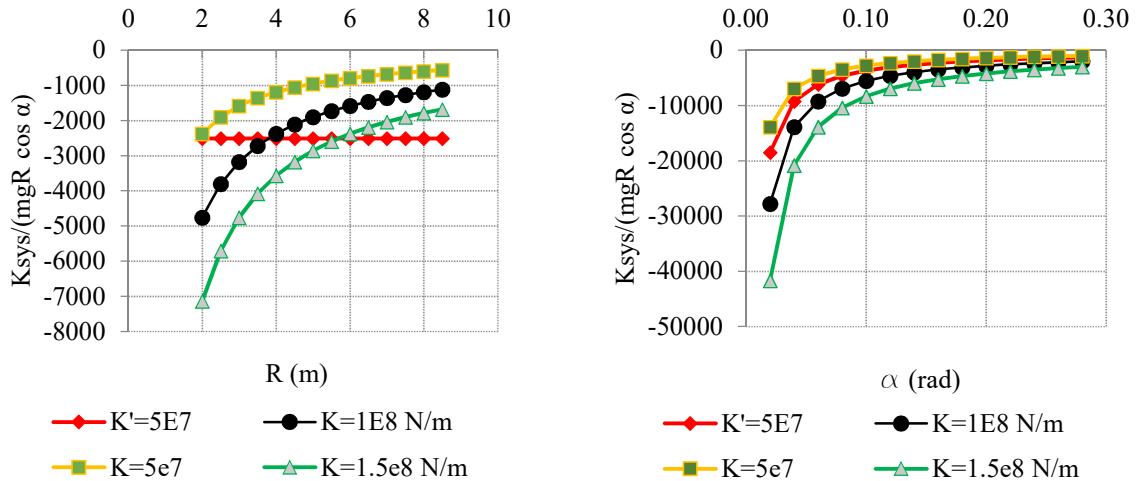
Figure 13: Variation of the system stiffness K_{sys} depending on the geometric parameters and on the values of single spring K ($\beta=1$) or spring bed stiffness K': $\alpha=0.15$ rad (a) and R=2.5 m (b).

6 LIMITATIONS OF THE METHOD

The illustrated method, for which it is possible to identify a target value of the single restraint stiffness to promote a self-centered (oscillatory) restrained motion, has some limitations, mainly related to correctly define the stiffness of transverse masonry walls. Indeed, the behavior of masonry is non-linear, but in this work only constant (for each sign of rotation) values of stiffness have been considered. Moreover, the determination of the elastic stiffness is not easy, inasmuch before an earthquake the diagonal cracks on transverse walls are generally unknown. Furthermore, if a portion of transverse walls rotates about a plastic hinge together with the rocking wall, their stiffness obviously does not affect motion. In this case, the role of transverse walls is only related to an increased masonry volume, an increased radius vector (of the complex system wall + transverse walls) and consequently a reduction of frequency parameter.

7 CONCLUSIONS

The model assumed in the paper simulates the behavior of a masonry wall connected to transverse walls and/or steel tie-rods, very frequently adopted as safety measure against out-of-plane modes due to seismic actions. From the system rotational stiffness, found for a Winkler-type model and for a single restraint, the resonance condition of the horizontally restrained block has been defined. The unilateral (restraint acting in only one direction of rotation) and the bilateral cases (restraints with similar stiffness in both directions) have been discussed. Real earthquakes, sine pulses or Ricker's wavelets were assumed as input parameters, obtaining results both for dimensionless parameters and for a real masonry façade. It is found that in the bilateral case the response is more predictable, as response spectra are generally monotonic curves able to enhance the response with a sensitive reduction of amplitude rotation. In particular, the effect of horizontal restraints is beneficial for the range of frequency parameters valid for typical masonry walls. These considerations allow to define a design strategy for ensure the rocking stability of restrained masonry walls, through a self-centered (oscillatory) rocking behavior. Indeed, once that the transverse stiffness of the wall is defined, it is straightforward to determine the value of K that equates the normalized system stiffness. From this values, dynamic analyses

have to be performed to draw rocking spectra in order to estimate the safety coefficient reached with the anti-seismic intervention.

ACKNOWLEDGEMENT

REFERENCES

[1]   DMI, "Decreto del Ministro delle Infrastrutture 14 gennaio 2008. Approvazione delle nuove norme tecniche per le costruzioni." Gazzetta Ufficiale della Repubblica Italiana, n. 29 del 4 febbraio 2008, Supplemento Ordinario n. 30, 2008.

[2]   CMIT, "Circolare del Ministro delle Infrastrutture e dei Trasporti 2 febbraio 2009, n. 617, contenente le Istruzioni per l'applicazione delle 'Nuove norme tecniche per le costruzioni' di cui al DM 14 gennaio 2008." Gazzetta Ufficiale della Repubblica Italiana n. 47 del 26 febbraio 2009, Supplemento Ordinario n. 27, 2009.

[3]   L. Giresini, "Energy-based method for identifying vulnerable macro-elements in historic masonry churches," *Bull. Earthq. Eng.*, vol. 14, no. 3, pp. 919–942, 2016.

[4]   L. Giresini, M. Fragiacomo, and P. B. Lourenço, "Comparison between rocking analysis and kinematic analysis for the dynamic out-of-plane behavior of masonry walls," *Earthq. Eng. Struct. Dyn.*, vol. 44, no. 13, pp. 2359–2376, Oct. 2015.

[5]   M. Sassu, "The Reinforced Cut Wall (RCW): A Low-Cost Base Dissipator for Masonry Buildings," *Earthq. Spectra*, vol. 22, no. 2, pp. 533–554, 2006.

[6]   I. N. Psycharis, D. Y. Papastamatiou, and A. P. Alexandris, "Parametric investigation of the stability of classical columns under harmonic and earthquake excitations," *Earthq. Eng. Struct. Dyn.*, vol. 29, no. 8, pp. 1093–1109, 2000.

[7]   G. W. Housner, "The behavior of inverted pendulum structures during earthquakes," *Bull. Seismol. Soc. Am.*, vol. 53, no. 2, pp. 403–417, 1963.

[8]   N. Makris and M. F. Vassiliou, "Dynamics of the Rocking Frame with Vertical Restrainers," *J. Struct. Eng.*, vol. 141, no. 10, 2015.

[9]   L. Giresini and M. Sassu, "Horizontally restrained rocking blocks: evaluation of the role of boundary conditions with static and dynamic approaches," *Bull. Earthq. Eng.*, vol. 15, no. 1, pp. 385–410, 2017.

[10]   L. Giresini, M. Fragiacomo, and M. Sassu, "Rocking analysis of masonry walls interacting with roofs," *Eng. Struct.*, vol. 116, pp. 107–120, Jun. 2016.

[11]   A. De Falco, L. Giresini, and M. Sassu, "Temporary preventive seismic reinforcements on historic churches: numerical modeling of San Frediano in Pisa," *Appl. Mech. Mater.*, vol. 352, 2013.

[12]   M. Andreini, A. De Falco, L. Giresini, and M. Sassu, "Collapse of the historic city walls of Pistoia (Italy): Causes and possible interventions," *Appl. Mech. Mater.*, vol. 351–352, 2013.

[13]   I. N. Psycharis, M. Fragiadakis, and I. Stefanou, "Seismic reliability assessment of classical columns subjected to near-fault ground motions," *Earthq. Eng. Struct. Dyn.*, vol. 42, no. 14, pp. 2061–2079, 2013.

[14]   C. Casapulla, "On the resonance conditions of rigid rocking blocks," *Int. J. Eng. Technol.*,

vol. 7, no. 2, pp. 760–771, 2015.

[15] C. Casapulla, P. Jossa, and A. Maione, "Rocking motion of a masonry rigid block under seismic actions: a new strategy based on the progressive correction of the resonance response," *Ing. Sismica*, vol. 27, no. 4, pp. 35–48, 2010.

[16] C. Casapulla and A. Maione, "Free damped vibrations of rocking rigid blocks as uniformly accelerated motions," *Int. J. Struct. Stab. Dyn.*, vol. 0, 2016.

[17] N. Makris and Y. S. Roussos, "Rocking response of rigid blocks under near-source ground motions," *Geotechnique*, vol. 50, p. 243, 2000.

[18] J. Zhang and N. Makris, "Rocking Response of Free-Standing Blocks under Cycloidal Pulses," *J. Eng. Mech.*, vol. 127, no. 5, 2001.

[19] N. Ricker, "Wavelet functions and their polynomials," *Geophysics*, vol. 9, p. 314, 1944.

[20] M. Apostolou, G. Gazetas, and E. Garini, "Seismic response of slender rigid structures with foundation uplifting," *Soil Dyn. Earthq. Eng.*, vol. 27, no. 7, pp. 642–654, 2007.

[21] G. I. Barenblatt, *Scaling, self-similarity, and intermediate asymptotics*. Mathematics, Cambridge Texts in Applied, series no 14, 1996.

[22] J. R. Dormand and P. J. Prince, "A family of embedded Runge-Kutta formulae," *J. Comput. Appl. Math.*, vol. 6, no. 1, pp. 19–26, 1980.

[23] N. Makris and M. F. Vassiliou, "Planar rocking response and stability analysis of an array of free-standing columns capped with a freely supported rigid beam," *Earthq. Eng. Struct. Dyn.*, vol. 42, p. 431, 2013.

[24] A. Brignola, S. Frumento, S. Lagomarsino, and S. Podestà, "Identification of Shear Parameters of Masonry Panels Through the In-Situ Diagonal Compression Test," *Int. J. Archit. Herit.*, vol. 3, no. 1, pp. 52–73, 2008.